J Therm Anal Calorim (2010) 102:1087–1093
DOI 10.1007/s10973-010-0688-x

Thermodynamic properties and heat capacities of Co $(BTC)_{1/3}$ (DMF) (HCOO)

Chun-Hong Jiang · Li-Fang Song · Jian Zhang · Li-Xian Sun · Fen Xu · Fen Li · Qing-Zhu Jiao · Zhen-Gang Sun · Yong-Heng Xing · Yong Du · Ju-Lan Zeng · Zhong Cao

Received: 29 October 2009 / Accepted: 14 January 2010 / Published online: 6 February 2010

Abstract A novel metal organic framework [Co $(BTC)_{1/3}$ (DMF) $(HCOO)]_n$ (CoMOF, BTC = 1,3,5-benzene tricarboxylate, DMF = *N*,*N*-dimethylformamide) has been synthesized solvothermally and characterized by single crystal X-ray diffraction, X-ray powder diffraction, and FT-IR spectra. The molar heat capacity of the compound was measured by modulated differential scanning calorimetry (MDSC) over the temperature range from 198 to 418 K for the first time. The thermodynamic parameters such as entropy and enthalpy versus 298.15 K based on the above molar heat capacity were calculated. Moreover, a four-step sequential thermal decomposition mechanism for the CoMOF was investigated through the thermogravimetry and mass spectrometer analysis (TG-DTG-MS) from 300 to 800 K. The apparent activation energy of the first decomposition step of the compound was calculated by the Kissinger method using experimental data of TG analysis.

Keywords Apparent activation energy · Co · MDSC · Molar heat capacity · Metal organic frameworks · TG

Introduction

Permanently porous metal-organic framework (MOF) materials are of tremendous current interest because of both their well-defined, low-density structures and their enormous potential in applications such as gas storage [1–4], catalysis [5], and separations [6]. The ability to synthesize MOFs with various organic linkers and metal joints provides great flexibility in tailoring the porous material to have specific physical characteristics and chemical functionalities. Furthermore, polynuclear cobalt complexes have been the subject of intensive study owing to their formation of diverse innovative structural networks, including chains, sheets, and matrices. There is also evidence that Cobalt complexes in polymer matrices show relatively interesting chemical and catalytic reactivity toward various small gas molecules [7].

Heat capacity is one of the most fundamental thermodynamic properties of substances in chemistry and engineering. Modulated differential scanning calorimetry (MDSC) is one of the easier and more accurate methods for determining heat capacity, and this method has been greatly developed for directly determining heat capacities for various materials isothermally and non-isothermally [8–13].

C.-H. Jiang · L.-F. Song · J. Zhang · L.-X. Sun (✉) · F. Li
Materials and Thermochemistry Laboratory, Dalian Institute of Chemical Physics, Chinese Academy of Sciences,
457 Zhongshan Road, 116023 Dalian,
People's Republic of China
e-mail: lxsun@dicp.ac.cn

F. Xu (✉) · Q.-Z. Jiao · Z.-G. Sun · Y.-H. Xing
Fac. Chem. and Chem. Engn., Liaoning Normal University,
Dalian 116029, People's Republic of China
e-mail: xufen@lnnu.edu.cn

C.-H. Jiang · L.-F. Song
Graduate School of the Chinese Academy of Sciences, Beijing
100049, People's Republic of China

Y. Du
State Key Laboratory of Powder Metallurgy, Central South
University, Changsha 410083, People's Republic of China

J.-L. Zeng · Z. Cao
School of Chemistry and Environmental Engineering, Changsha
University of Science and Technology, Changsha 410076,
People's Republic of China

In this study, we reported one novel cobalt metal organic framework [Co $(BTC)_{1/3}$ (DMF) (HCOO)]$_n$ (CoMOF, BTC = 1,3,5-benzene tricarboxylate, DMF = *N*,*N*-dimethylformamide). The molar heat capacity of the compound was measured by MDSC from 198 to 418 K, and the thermodynamic parameters such as entropy and enthalpy were also calculated. The thermal decomposition characteristics of this compound were investigated by TG-DTG-MS techniques at the temperature range from 300 to 800 K.

Experimental

All materials were commercially available and were of analytical grade unless stated elsewhere.

Sample preparation

[Co $(BTC)_{1/3}$ (DMF) (HCOO)]$_n$ was prepared by solvothermal reaction. $Co(NO_3)_2 \cdot 6H_2O$ (0.87 g, 3 mmol) and H_3BTC (0.42 g, 2 mmol) were dissolved in DMF/H_2O (2:1 by volume, 24 mL). Then, the mixture was sealed in a 50-mL Teflon-lined stainless steel autoclave and heated at 120 °C for 48 h, then cooled naturally to room temperature. The resulting purple block-shaped crystals were isolated by filtration and washed thoroughly with DMF, and finally dried at 50 °C overnight. Yield: 56%, based on Co.

Characterization

The single crystal X-ray diffraction intensities were collected over a SMART APEX II-CCD diffractometer equipped with a fine-focus sealed tube with graphite monochromated MoK_α ($\lambda = 0.71073$ Å) radiation source at 293 K. The structures were solved by direct methods and refined by full-matrix least-squares method implemented in SHELXTL-97 [14]. All the non-hydrogen atoms were refined anisotropically. Hydrogen atoms were added theoretically. FT-IR spectra were recorded on a Nicolet 380 FT-IR spectrometer using KBr pellet in the wavelength range of 4,000–400 cm^{-1}.

Crystal data for the compound were as follows: trigonal system, P-3 (147), $a = 13.969(4)$, $b = 13.969(4)$, $c = 8.096(5)$, $\alpha = 90.00$, $\beta = 90.00$, $\gamma = 120.00$, final $R_1 = 0.0506$, and $wR_2 = 0.1507$. Figure 1 shows the X-ray crystal structure of the compound along the *c* axis. The molar mass of the compound is 246.08.

Elemental analysis (%) calculated for this compound: C 34.36, H 3.52, N 5.62; found: C 34.17, H 3.69, N 5.69.

FT-IR: 3,040–3,650 cm^{-1}, ν(O–H); 2,938 cm^{-1}, ν_{as}(C–H); 2,880 cm^{-1}, ν_s(C–H); 1,450–1,600 cm^{-1}, ν(aromatic C=C); 1,627 cm^{-1}, ν_{as}(COO); 1,382 cm^{-1}, ν_s(COO).

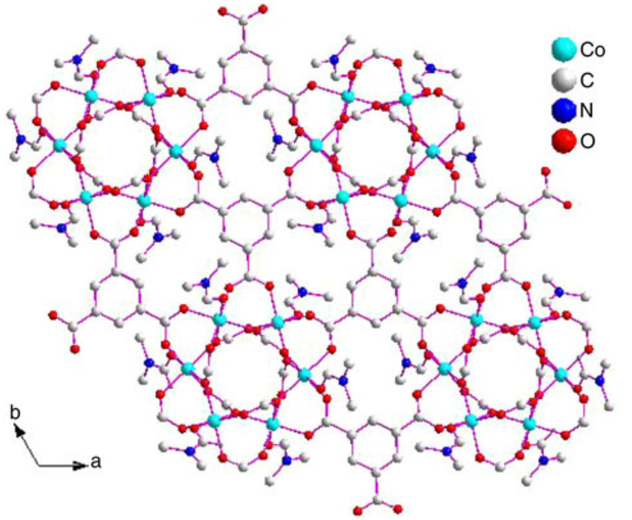

Fig. 1 X-ray crystal structure of CoMOF along the *c* axis. All hydrogen atoms are omitted for clarity

Heat capacity measurement

Heat capacity measurements were performed on DSC Q1000 (T-zero DSC-technology, TA Instruments Inc., USA) with a heating rate of 10 K min^{-1}. Dry high purity nitrogen (99.999%) was used as purge gas at a flow rate of 50 mL min^{-1} through the DSC cell. And a mechanical cooling system was used for the experimental measurement. The temperature scale of the instrument was initially calibrated in the standard DSC mode, using the extrapolated onset temperatures of the melting of indium (429.75 K) as described in our previous articles [11–13]. The energy scale was calibrated with the heat of fusion of indium (28.45 J g^{-1}). The heat capacity calibration was made by running a standard sapphire (Al_2O_3) at the experimental temperature. The accuracy of MDSC is established by comparing the measured heat capacity of standard sapphire with previously reported values [15]. The calibration method and the experiment were performed at the same conditions as follows: (1) sampling interval: 1.00 s/pt; (2) zero heat flow at 253.15 K; (3) equilibrate at 133.15 K; (4) modulate temperature amplitude of ±0.5 K with period of 100 s; (5) isothermal for 5 min; (6) temperature ramp at 5 K min^{-1} to 453 K. The constants of heat capacity for the MDSC: $K_{total} = 1.024$; $K_{reversible} = 1.019$.

The masses of the reference and sample pans with lids were measured to be within 30 ± 0.05 mg. Samples were crimped in non-hermetic aluminum pans with lids. Sample mass was weighed on a METTLER TOLEDO electrobalance (AB135-S, Classic) with an accuracy of (±0.01 mg).

Thermal analysis

A thermogravimetric analyzer (Model: Setsys 16/18, SETARAM Co., France) was used for TG measurement of this compound under air atmosphere from 300 to 800 K. Several experiments were carried out at the heating rates of $\beta = 10, 12.5, 15, 17.5, 20\ \mathrm{K\ min^{-1}}$, and the flow rate of air was 45 mL $\mathrm{min^{-1}}$. The mass of the compound was about 10 mg. The TG equipment was calibrated by the $CaC_2O_4 \cdot H_2O$ (99.9%). Mass spectra (MS) were performed on a Multicomponent Online Gas Analyzer GAM 200.

Results and discussion

Heat capacity

Three reduplicate experiments (test 1, test 2, and test 3), the average, and the standard deviation of this compound are given in Table 1, and the mass of the compound in the reduplicate experiments are 6.92, 7.02, and 7.23 mg. The experimental standard deviations are below 0.021 J $\mathrm{K^{-1}\ g^{-1}}$, and this show reasonably good reproducibility in the experimental temperature range from 198 to 418 K. The experimental molar heat capacities curve of the compound versus temperature is shown in Fig. 2. The heat capacity of the sample increases continuously with the increasing temperature from 198 to 418 K. No phase transition or thermal anomaly was observed in the experimental temperature range. This indicates that the sample is stable in this temperature region.

The experimental and calculated molar heat capacities data are listed in Table 2. The molar heat capacities of the sample are fitted to the following polynomial equation of heat capacities ($C_{p,m}$) with reduced temperature (X) by means of the least square fitting:

From $T = (198\text{–}418)$ K

$$C_{p,m}\left[\mathrm{J\ mol^{-1}\ K^{-1}}\right] = 279.0 + 67.11X - 7.012X^2 - 0.9069X^3 + 1.081X^4 \quad (1)$$

where $X = (T - 308)/110$, and T is the experimental temperature, 308 is obtained from polynomial $(T_{max} + T_{min})/2$, 110 is obtained from polynomial $(T_{max} - T_{min})/2$, T_{max} is the upper limit (418 K) of the above temperature region, T_{min} is the lower limit (198 K) of the above temperature region. The correlation coefficient of the fitting, $R^2 = 0.99965$. The relative deviations of all the experimental points from the fitting heat capacity values are within ±0.44% in Table 2. Relative deviations have been calculated by the following equation:

Table 1 The data of three reduplicate experiments for CoMOF

T/K	$C_{p,m}$(exp)/J $\mathrm{K^{-1}\ g^{-1}}$				Standard deviation/ J $\mathrm{K^{-1}\ g^{-1}}$
	Test 1	Test 2	Test 3	Average	
198	0.8415	0.8417	0.8241	0.8358	0.010
203	0.8624	0.8627	0.8415	0.8555	0.012
208	0.8768	0.8777	0.8544	0.8696	0.013
213	0.8907	0.8906	0.8659	0.8824	0.014
218	0.9036	0.9042	0.8779	0.8952	0.015
223	0.9172	0.9177	0.8909	0.9086	0.015
228	0.9327	0.9335	0.9040	0.9234	0.017
233	0.9478	0.9486	0.9173	0.9379	0.018
238	0.9617	0.9630	0.9301	0.9516	0.018
243	0.9778	0.9792	0.9448	0.9673	0.019
248	0.9946	0.9957	0.9589	0.9831	0.021
253	1.009	1.010	0.9727	0.9972	0.021
258	1.015	1.015	0.9845	1.005	0.018
263	1.019	1.022	0.9977	1.013	0.013
268	1.032	1.035	1.011	1.026	0.013
273	1.046	1.048	1.025	1.040	0.013
278	1.060	1.062	1.039	1.054	0.013
283	1.075	1.074	1.054	1.068	0.012
288	1.087	1.087	1.068	1.081	0.011
293	1.100	1.101	1.081	1.094	0.011
298	1.114	1.113	1.097	1.108	0.0095
303	1.126	1.126	1.109	1.120	0.0098
308	1.138	1.139	1.122	1.133	0.0095
313	1.149	1.150	1.135	1.145	0.0084
318	1.162	1.162	1.153	1.159	0.0052
323	1.174	1.174	1.171	1.173	0.0017
328	1.186	1.188	1.184	1.186	0.0020
333	1.198	1.199	1.199	1.199	0.00058
338	1.206	1.208	1.212	1.209	0.0031
343	1.216	1.218	1.223	1.219	0.0036
348	1.226	1.228	1.234	1.229	0.0042
353	1.238	1.241	1.246	1.242	0.0040
358	1.249	1.253	1.257	1.253	0.0040
363	1.261	1.266	1.269	1.265	0.0040
368	1.274	1.276	1.282	1.277	0.0042
373	1.281	1.285	1.290	1.285	0.0045
378	1.289	1.294	1.298	1.294	0.0045
383	1.296	1.303	1.306	1.302	0.0051
388	1.306	1.311	1.316	1.311	0.0050
393	1.318	1.323	1.328	1.323	0.0050
398	1.330	1.334	1.339	1.334	0.0045
403	1.342	1.346	1.353	1.347	0.0056
408	1.354	1.360	1.366	1.360	0.0060
413	1.366	1.371	1.377	1.371	0.0055
418	1.376	1.381	1.389	1.382	0.0066

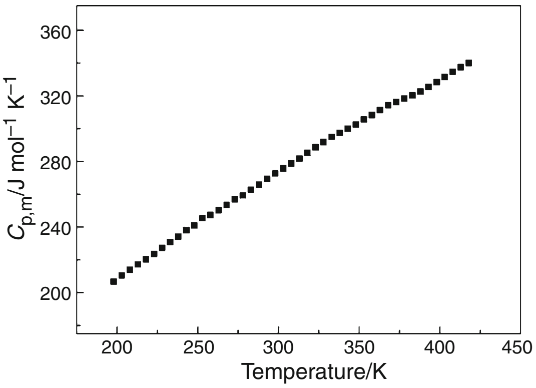

Fig. 2 Molar heat capacities ($C_{p,m}$) of CoMOF as a function of temperature

$$\mathrm{RD}\ (\%) = 100\left[C_{p,m}(\exp) - C_{p,m}(\mathrm{fit})\right]/C_{p,m}(\mathrm{fit}) \tag{2}$$

where $C_{p,m}$(exp) is the experimental molar heat capacity and $C_{p,m}$(fit) is the calculated heat capacity. Based on Eq. 1, the heat capacity of the compound at 298.15 K was calculated to be 272.9 J mol^{-1} K^{-1}.

Thermodynamic functions

Enthalpy and entropy of substances are basic thermodynamic functions. Through the polynomial representing heat capacity and the relationship between thermodynamic functions and heat capacity, the thermodynamic functions relative to the reference temperature of 298.15 K of this compound were calculated from 198 to 418 K with an interval of 5 K. The thermodynamic relationships are as follows:

$$H_T - H_{298.15} = \int_{298.15}^{T} C_{p,m}\,\mathrm{d}T \tag{3}$$

$$S_T - S_{298.15} = \int_{298.15}^{T} (C_{p,m}/T)\mathrm{d}T. \tag{4}$$

The calculated thermodynamic functions $[H_T - H_{298.15}]$ and $[S_T - S_{298.15}]$ are listed in Table 3. It can be seen that both of the thermodynamic functions $[H_T - H_{298.15}]$ and $[S_T - S_{298.15}]$ of the compound increase with increasing temperature in a continuous manner in the temperature range from 198 to 418 K.

Table 2 The experimental and calculated molar heat capacities of CoMOF

T/K	$C_{p,m}$(exp)/ J K^{-1} mol^{-1}	$C_{p,m}$(fit)/ J K^{-1} mol^{-1}	RD/%	*T*/K	$C_{p,m}$(exp)/ J K^{-1} mol^{-1}	$C_{p,m}$(fit)/ J K^{-1} mol^{-1}	RD/%
198	206.67	206.87	−0.10	313	281.68	282.04	−0.13
203	210.53	210.24	0.14	318	285.21	285.04	0.058
208	214.00	213.62	0.18	323	288.65	288.02	0.22
213	217.14	217.00	0.066	328	291.85	290.97	0.30
218	220.30	220.38	−0.036	333	294.97	293.88	0.37
223	223.59	223.76	−0.076	338	297.43	296.77	0.22
228	227.23	227.14	0.042	343	299.97	299.63	0.12
233	230.80	230.50	0.13	348	302.51	302.45	0.021
238	234.17	233.87	0.13	353	305.55	305.25	0.098
243	238.02	237.21	0.34	358	308.34	308.02	0.10
248	240.91	240.55	0.15	363	311.37	310.76	0.20
253	243.40	243.87	0.19	368	314.33	313.47	0.27
258	247.27	247.18	0.037	373	316.30	316.15	0.045
263	250.25	250.46	−0.084	378	318.35	318.81	−0.15
268	253.48	253.73	−0.10	383	320.31	321.44	−0.35
273	256.84	256.98	−0.053	388	322.61	324.05	−0.44
278	259.29	260.20	−0.35	393	325.56	326.64	−0.33
283	262.73	263.40	−0.25	398	328.35	329.20	−0.26
288	265.93	266.57	−0.24	403	331.47	331.75	−0.083
293	269.21	269.72	−0.19	408	334.67	334.21	0.12
298	272.66	272.84	−0.068	413	337.46	336.78	0.20
303	275.69	275.94	−0.088	418	340.08	339.27	0.24
308	278.81	279.00	−0.069				

Table 3 Calculated thermodynamic function data of CoMOF

T/K	$H_T - H_{298.15}$/ kJ mol^{-1}	$S_T - S_{298.15}$/ J K^{-1} mol^{-1}	T/K	$H_T - H_{298.15}$/ kJ mol^{-1}	$S_T - S_{298.15}$/ J K^{-1} mol^{-1}
198	−24.07	−97.46	308	2.718	8.966
203	−23.03	−92.27	313	4.121	13.48
208	−21.97	−87.11	318	5.539	17.97
213	−20.89	−82.00	323	6.971	22.44
218	−19.80	−76.92	328	8.419	26.89
223	−18.69	−71.89	333	9.881	31.31
228	−17.56	−66.88	338	11.36	35.71
233	−16.42	−61.92	343	12.85	40.09
238	−15.26	−56.99	348	14.35	44.45
243	−14.08	−52.09	353	15.87	48.78
248	−12.89	−47.22	358	17.41	53.10
253	−11.67	−42.38	363	18.95	57.39
258	−10.45	−37.58	368	20.51	61.66
263	−9.202	−32.80	373	22.09	65.91
268	−7.942	−28.06	378	23.68	70.14
273	−6.665	−23.34	383	25.26	74.35
278	−5.372	−18.64	388	26.89	78.53
283	−4.063	−13.98	393	28.52	82.70
288	−2.738	−9.339	398	30.16	86.85
293	−1.397	−4.726	403	31.81	90.97
298	−0.04093	−0.1373	408	33.47	95.08
298.15	0	0	413	35.15	99.16
303	1.331	4.427	418	36.84	103.2

TG-DTG-MS results

The TG-DTG-MS curves (Fig. 3) of this compound show that a four-stage mass loss occurs in the temperature range from 442 to 675 K. The first mass loss starts at 442 K and is about 14.7% (calculated 14.1%) likely due to the loss of one-sixth molecule of DMF and a half of HCOO. The MS curve shows that the gas degradation products are mainly H_2O ($m/z = 18$), CO ($m/z = 28$), and NO ($m/z = 30$). The second stage takes place between 514 and 553 K and is accompanied by 9.0% mass loss, and it is attributed to the loss of one-fourth of HCOO and one-sixth of DMF (calculated 9.5%). The gas products of the stage are mainly H_2O ($m/z = 18$), CO ($m/z = 28$), and NO ($m/z = 30$). The third mass loss is 14.5% (from 553 to 592 K) and due to one-third of DMF and one-fourth of HCOO (calculated 14.4%), with the gas oxidation products are H_2O ($m/z = 18$), CO_2 ($m/z = 44$), and NO_2 ($m/z = 46$) as shown in MS curve. The last stage is from 592 to 675 K and about 30.6% mass loss (calculated 31.5%), and which is decomposed to cobalt oxide, with the gas oxidation products are H_2O ($m/z = 18$), CO_2 ($m/z = 44$), NO ($m/z = 30$), and NO_2 ($m/z = 46$). The overall mass loss of the compound is about 68.8% in accord with the calculated percentage (69.5%). The possible mechanism of the thermal decomposition can be traced as follows:

$$\mathrm{Co\ (BTC)_{1/3}\ (C_3H_7NO)\ (HCOO)} \xrightarrow[-1/6\mathrm{DMF}-1/2\mathrm{HCOO}]{442-514\ \mathrm{K}}$$

$$\mathrm{Co\ (BTC)_{1/3}\ (C_3H_7NO)_{5/6}\ (HCOO)_{1/2}} \xrightarrow[-1/6\mathrm{DMF}-1/4\mathrm{HCOO}]{514-553\ \mathrm{K}}$$

$$\mathrm{Co\ (BTC)_{1/3}\ (C_3H_7NO)_{2/3}\ (HCOO)_{1/4}} \xrightarrow[-1/3\mathrm{DMF}-1/4\mathrm{HCOO}]{553-592\ \mathrm{K}}$$

$$\mathrm{Co\ (BTC)_{1/3}\ (C_3H_7NO)_{1/3}} \xrightarrow[-1/3\mathrm{DMF}-\mathrm{C_3HO}]{592-675\ \mathrm{K}} \mathrm{CoO}.$$

The CoMOF is stable to 442 K according to the TG curve. The calculation by SOLV within PLATON indicated that in this compound, the solvent-accessible volume is approximately 33.7 Å^3 per unit cell volume (1,368.1 Å^3), thus representing 2.5% of the total cell volume. Further investigations based on this compound for other purposes, like hydrogen storage and gas sensor, are now underway in our group.

Thermal kinetic study for TG analysis

Thermal kinetic parameter for the first-step decomposition of this CoMOF was analyzed using Kissinger method [16],

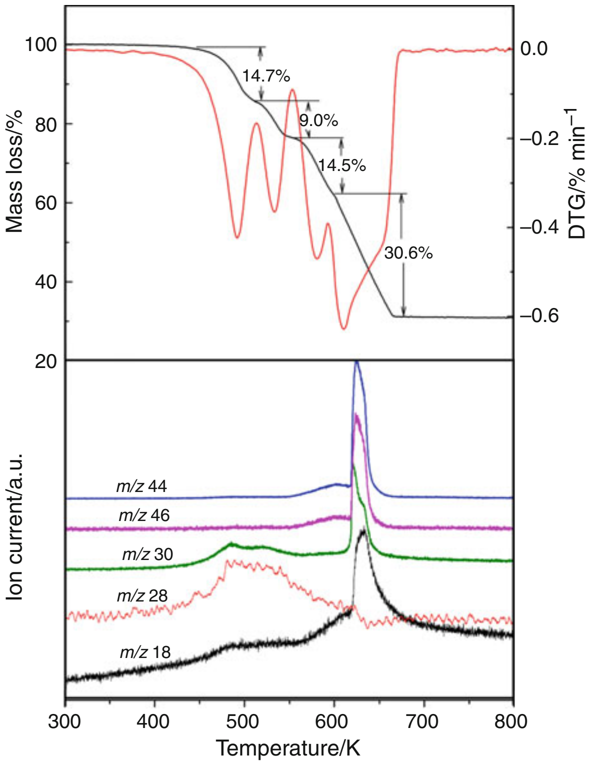

Fig. 3 TG-DTG-MS curves of CoMOF under air atmosphere at 10 K min^{-1}

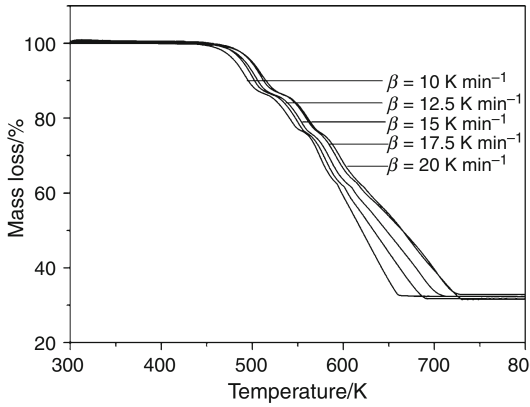

Fig. 4 TG curves of CoMOF under air atmosphere at 10, 12.5, 15, 17.5, 20 K min^{-1}

which has been widely applied to estimate the apparent activation energy. Figure 4 shows the TG curves of the CoMOF measured in air atmosphere from 300 to 800 K with the heating rate of 10, 12.5, 15, 17.5, 20 K min^{-1}, respectively. The basic data (β, T_p) taken from the TG curves are used in the following Kissinger equation:

$$\ln(\beta/T_\mathrm{p}^2) = \ln(AR/E) - E/RT_\mathrm{p} \tag{5}$$

where β is the heating rate, T_p peak temperature of the corresponding DTG curves, A pre-exponential factor, R gas constant, and E apparent activation energy. Plot of $\ln(\beta/T_\mathrm{p}^2)$ versus $1/T_\mathrm{p}$ should fit to a straight line with a slope of $-E/R$. Such plot for the first-step decomposition of the CoMOF is exhibited in Fig. 5. The E value and A value of the compound were calculated to be 72.84 kJ mol^{-1} and 1.986×10^7, respectively.

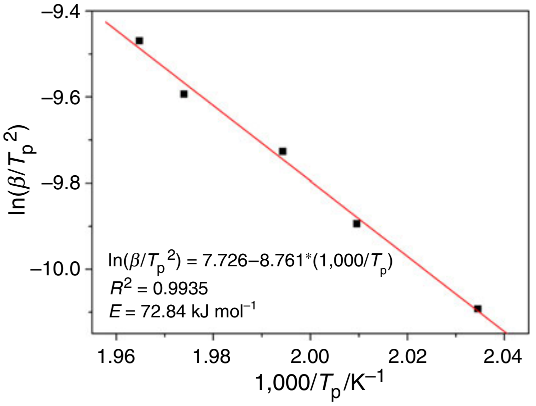

Fig. 5 Fitting using Kissinger method for the corresponding DTG curves

Conclusions

In this study, one novel Cobalt metal organic framework has been solvothermally synthesized and characterized. The molar heat capacities of the compound were measured by MDSC for the first time. The heat capacity of the compound at 298.15 K was calculated to be 272.9 J mol^{-1} K^{-1}. The thermodynamic function data (enthalpy and entropy) relative to the reference temperature (298.15 K) were calculated in the temperature range from 198 to 418 K. Moreover, the thermal stability and its decomposition mechanism of the compound were investigated by TG-DTG-MS analysis. A four-stage mass loss occurs in the temperature range from 442 to 675 K. With the decomposition of the framework, the DMF, HCOO, and BTC are partly and continuously decomposed during the mass loss stages. The apparent activation energy of the first decomposition step of the compound was calculated to be 72.84 kJ mol^{-1}, by the Kissinger method using experimental data of TG analysis.

Acknowledgements The authors gratefully acknowledge the financial support for this study from the National Natural Science Foundation of China (No. 2083309, 20873148, 50671098 and U0734005), the National High Technology Research and Development Program of China (2007AA05Z115 and 2007AA05Z102), the National Basic Research Program (973 program) of China (2010CB631303), and IUPAC (Project No. 2008-006-3-100).

References

1. Wong-Foy AG, Matzger AJ, Yaghi OM. Exceptional H-2 saturation uptake in microporous metal-organic frameworks. J Am Chem Soc. 2006;128:3494–5.
2. Fletcher AJ, Thomas KM, Rosseinsky MJ. Flexibility in metal-organic framework materials: impact on sorption properties. J Solid State Chem. 2005;178:2491–510.
3. Navarro JAR, Barea E, Salas JM, Masciocchi N, Galli S, Sironi A, et al. H_2, N_2, CO, and CO_2 sorption properties of a series of robust sodalite-type microporous coordination polymers. Inorg Chem. 2006;45:2397–9.
4. Latroche M, Surble S, Serre C, Mellot-Draznieks C, Llewellyn PL, Lee JH, et al. Hydrogen storage in the giant-pore metal-organic frameworks MIL-100 and MIL-101. Angewandte Chem-Int Ed. 2006;45:8227–31.
5. Wu CD, Hu A, Zhang L, Lin WB. Homochiral porous metal-organic framework for highly enantioselective heterogeneous asymmetric catalysis. J Am Chem Soc. 2005;127:8940–1.
6. Chen BL, Liang CD, Yang J, Contreras DS, Clancy YL, Lobkovsky EB, et al. A microporous metal-organic framework for gas-chromatographic separation of alkanes. Angewandte Chem-Int Ed. 2006;45:1390–3.
7. Jalbout AF, Li XH, Hassan MR, Hossain GMG. Construction of novel coordination polymers with simple ligands. Transit Met Chem. 2008;33:597–603.
8. Reading M, Elliot D, Hill V. Some aspects of the theory and practise of modulated differential scanning calorimetry. In: Proceedings of the 21st North American Thermal Analysis Society Conference. 1992, pp. 145–50.
9. Wunderlich B. The contributions of MDSC to the understanding of the thermodynamics of polymers. J Therm Anal Calorim. 2006;85:179–87.
10. Chau J, Garlicka I, Wolf C, Teh J. Modulated DSC as a tool for polyethylene structure characterization. J Therm Anal Calorim. 2007;90:713–9.
11. Qi YN, Xu F, Ma HJ, Sun LX, Zhang J, Jiang T. Thermal stability and glass transition behavior of PANI/gamma-Al_2O_3 composites. J Therm Anal Calorim. 2008;91:219–23.
12. Qiu SJ, Chu HL, Zhang J, Qi YN, Sun LX, Xu F. Heat capacities and thermodynamic properties of CoPc and CoTMPP. J Therm Anal Calorim. 2008;91:841–8.
13. Zhang J, Zeng JL, Liu YY, Sun LX, Xu F, You WS, et al. Thermal decomposition kinetics of the synthetic complex Pb(1, 4-BDC)center dot(DMF)(H_2O). J Therm Anal Calorim. 2008;91: 189–93.
14. Sheldrick GM. SHELX97. Program for crystal structure refinement. 1997.
15. Archer DG. Thermodynamic properties of synthetic sapphire (Alpha-Al_2O_3), Standard Reference Material 720 and the effect of temperature-scale differences on thermodynamic properties. J Phys Chem Ref Data. 1993;22:1441–53.
16. Kissinger HE. Reaction kinetics in differential thermal analysis. Anal Chem. 1957;29:1702–6.